On-chip measurements of Brownian relaxation vs. concentration of 40nm magnetic beads

Østerberg, Frederik Westergaard; Rizzi, Giovanni; Hansen, Mikkel Fougt

Published in:
Journal of Applied Physics

Link to article, DOI:
10.1063/1.4769796

Publication date:
2012

Document Version
Publisher's PDF, also known as Version of record

AIP | Journal of Applied Physics

On-chip measurements of Brownian relaxation vs. concentration of 40nm magnetic beads

Frederik Westergaard Østerberg, Giovanni Rizzi, and Mikkel Fougt Hansen

Citation: J. Appl. Phys. **112**, 124512 (2012); doi: 10.1063/1.4769796
View online: http://dx.doi.org/10.1063/1.4769796
View Table of Contents: http://jap.aip.org/resource/1/JAPIAU/v112/i12
Published by the American Institute of Physics.

JOURNAL OF APPLIED PHYSICS **112**, 124512 (2012)

On-chip measurements of Brownian relaxation vs. concentration of 40 nm magnetic beads

Frederik Westergaard Østerberg,[a] Giovanni Rizzi, and Mikkel Fougt Hansen[b]
Department of Micro- and Nanotechnology, Technical University of Denmark, DTU Nanotech, Building 345B, DK-2800 Kongens Lyngby, Denmark

(Received 21 September 2012; accepted 16 November 2012; published online 20 December 2012)

We present on-chip Brownian relaxation measurements on a logarithmic dilution series of 40 nm beads dispersed in water with bead concentrations between 16 μg/ml and 4000 μg/ml. The measurements are performed using a planar Hall effect bridge sensor at frequencies up to 1 MHz. No external fields are needed as the beads are magnetized by the field generated by the applied sensor bias current. We show that the Brownian relaxation frequency can be extracted from fitting the Cole-Cole model to measurements for bead concentrations of 64 μg/ml or higher and that the measured dynamic magnetic response is proportional to the bead concentration. For bead concentrations higher than or equal to 500 μg/ml, we extract a hydrodynamic diameter of 47(1) nm for the beads, which is close to the nominal bead size of 40 nm. Furthermore, we study the signal vs. bead concentration at a fixed frequency close to the Brownian relaxation peak and find that the signal from bead suspensions with concentrations down to 16 μg/ml can be resolved. © *2012 American Institute of Physics*. [http://dx.doi.org/10.1063/1.4769796]

I. INTRODUCTION

Magnetic beads have proven useful for biosensing as most biological samples are non-magnetic such that magnetic beads can be manipulated and detected independently of the sample chemistry. Furthermore, magnetic biosensors rely on magnetic methods for detecting the magnetic beads, which provide an electrical signal that can be directly read out. Among the typical methods for detecting magnetic beads are inductive methods,[1] fluxgates,[2] superconducting quantum interference device (SQUID) magnetometers,[3,4] and magnetoresistive sensors.[5–7] There are pros and cons for each method; for instance, SQUID magnetometers are very sensitive but are costly, require cryogenics and are not easily integrated with a sample preparation system. Magnetoresistive sensors are not as sensitive as SQUID magnetometers but they can be operated at room temperature, they are small in dimensions, they are potentially inexpensive and they can be integrated in lab-on-a-chip systems. Thus, magnetoresistive sensors are attractive for use in lab-on-a-chip magnetic biosensing platforms.

Magnetic beads have been used for biosensing in surface-based[8] and volume-based[1,9,10] assays. In a surface-based assay, the surfaces of both the sensor and the beads are functionalized such that the presence of the analyte results in specific binding of the beads to the sensor surface. In a volume-based assay, only the beads are functionalized prior to detection and the analyte modifies the hydrodynamic size of the beads, either due to its size[11] or by inducing bead agglutination.[1] The dispersion of hydrodynamic sizes for a magnetic bead ensemble can be characterized via Brownian relaxation measurements, which were first proposed for biosensing by Connolly and St Pierre.[12]

For volume-based bioassays, the limit of detection is sensitive to the bead concentration: for a high bead concentration, only a small fraction of the beads are affected by a given amount of analyte, whereas the opposite is the case for a low bead concentration. On the other hand, a low bead concentration results in a smaller dynamic range of analyte concentrations that can be detected. Thus, the bead concentration is an important parameter for the sensitivity and dynamic range for volume-based biosensing. For any readout principle for volume-based bioassays, it is therefore important to know its dependence on the bead concentration and the range of bead concentrations for which the magnetic dynamics can be reliably characterized.

In this study, we investigate the dependence of the on-chip measurements of the dynamic magnetic bead signal on the concentration of beads with a nominal diameter of 40 nm. The study is carried out using so-called planar Hall effect bridge (PHEB) sensors[13] currently being investigating for volume-based magnetic biodetection.[10] The sensors are integrated in a microfluidic system and do not rely on any external magnetic fields. We determine the lower limit of bead concentrations required for obtaining reliable measurements of the dynamic magnetic Brownian relaxation response and we also investigate the lowest bead concentration that can be detected by the present sensors.

II. THEORY

The magnetic field sensors used in the study are based on the anisotropic magnetoresistance (AMR) effect, which causes the resistivity to be largest when the current and applied magnetic field are parallel and lowest when they are orthogonal. The sensor geometry is composed of four segments to form a Wheatstone bridge as shown in Fig. 1. Here, the potential difference V_y in the y-direction is measured upon injection of a current I in the x-direction. The sensor

[a]Electronic address: Frederik.Osterberg@nanotech.dtu.dk.
[b]Electronic address: Mikkel.Hansen@nanotech.dtu.dk.

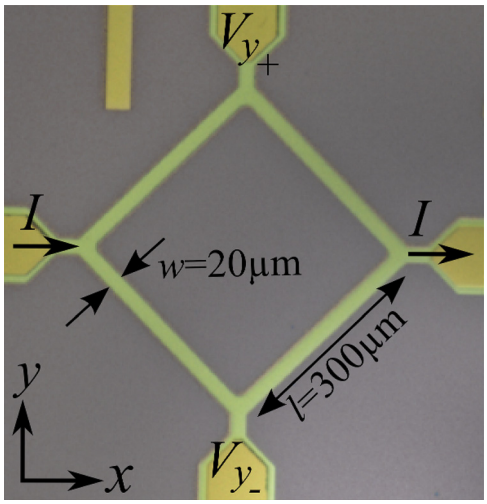

FIG. 1. Picture of sensor with definitions of dimensions. The bias current I is applied through the arms in the x-direction, while the potential difference V_y is measured across the y-direction. The length l and width w of a bridge segment are also shown.

consists of a ferromagnetic layer exhibiting the AMR effect, which is pinned along the positive x-direction by an antiferromagnetic layer. This ensures that the magnetization of the sensor is single domain and has a fixed orientation in the absence of external magnetic fields. It has recently been shown that the signal from the bridge structure shown in Fig. 1 is identical to that from a regular planar Hall effect sensor cross, except for a geometrical amplification.[13] To distinguish this particular geometry from other AMR sensor geometries, we have named sensors with this geometry planar Hall effect bridge sensors.

For low magnetic fields, the sensor signal is linear and given by[13]

$$V_y = IS_0H_y, \tag{1}$$

where S_0 is the low-field sensitivity and H_y is the magnetic field in the y-direction.

Measurements on magnetic bead suspensions are carried out without application of external magnetic fields. Instead, the magnetic beads are magnetized by the sensor self-field arising from the bias current passed through the sensor. For an alternating bias current $I(t) = I_{AC}\sin(2\pi ft)$, both the bias current and the field from the beads will oscillate at the frequency f of the bias current. As the sensor response due to the presence of magnetic beads is proportional to I^2, these will give rise to a signal oscillating at $2f$. The dynamic magnetic response of the magnetic beads is described by their complex susceptibility $\chi = \chi' - i\chi''$, where χ' and χ'' are the in-phase and out-of-phase magnetic susceptibilities of the beads, respectively. We have previously shown that the dynamic magnetic bead response for beads magnetized by the self-field can be detected using lock-in technique[10,14,15] and that the second harmonic in-phase and out-of-phase sensor signals V_2' and V_2'' for a PHEB sensor are given by[10]

$$V_2' = -2^{-3}I_{AC}^2S_0\gamma_1\chi'', \tag{2}$$

$$V_2'' = -2^{-3}I_{AC}^2S_0(\gamma_0 + \gamma_1\chi'), \tag{3}$$

where γ_0 is a constant that depends on the sensor stack and sensor geometry and γ_1 is a constant that depends on the sensor geometry and distribution of beads. Thus, the in-phase second harmonic sensor signal is proportional to the out-of-phase magnetic bead susceptibility and the out-of-phase second harmonic sensor signal depends linearly on the in-phase magnetic bead susceptibility.

A. Brownian relaxation of magnetic of beads

When a magnetic bead is placed in a magnetic field, the magnetization of the bead will align with the field either by internal flipping of the magnetic moment (Néel relaxation[16]) or by a physical rotation of the bead (Brownian relaxation[17]). For the beads used in this study, the Néel relaxation time is much longer than the Brownian relaxation time, which therefore dominates the relaxation dynamics of the beads. Brownian relaxation is characterized by the Brownian relaxation frequency,

$$f_B = \frac{k_BT}{6\pi\eta V_h}, \tag{4}$$

where k_BT is the thermal energy, η is the viscosity of the liquid in which the bead is suspended, and V_h is the hydrodynamic volume of the bead. The Brownian relaxation frequency is the frequency at which the phase-lag between the magnetic moment of the bead and the applied field is largest, meaning that a peak will appear in the out-of-phase magnetic susceptibility at $f = f_B$.

The complex susceptibility of a monodisperse ensemble of beads is described by the Debye theory.[18] The complex susceptibility of an ensemble of polydisperse beads is usually described by the empirical Cole-Cole model,[19]

$$\chi = \frac{\chi_0 - \chi_\infty}{1 + (if/f_B)^{1-\alpha}} + \chi_\infty, \tag{5}$$

where χ_0 and χ_∞ are the DC and high-frequency susceptibilities, respectively, and $0 \le \alpha \le 1$ is a measure of the polydispersity ($\alpha = 0$ for a monodisperse sample). The Cole-Cole model has been used for analyzing the data in the present work to extract f_B, α, and the DC and high-frequency susceptibilities.

III. EXPERIMENTAL

The geometric variables of the sensor are defined in Fig. 1. Each of the four branches in the sensor bridge used in the present study has a length of $l = 300$ μm and a width of $w = 20$ μm and was fabricated as follows: First, an 800 nm thick oxide was grown on a silicon wafer by wet oxidation. Then, the sensor stack Ta(3 nm)/$Ni_{80}Fe_{20}$(30 nm)/$Mn_{80}Ir_{20}$ (20 nm)/Ta(3 nm) was deposited in a Kurt J. Lesker Co. CMS-18 sputter system and defined by lift-off. During deposition, a magnetic field of 20 mT was applied to define the easy direction of the magnetization along the positive x-direction in Fig. 1. Electrical contacts to the sensors of Ti(5 nm)/Au(100 nm)/Pt(100 nm)/Ti(5 nm) were deposited by e-beam evaporation and defined by lift-off. Subsequently,

a protective coating of Ormocomp (Micro Resist Technology GmbH, Germany) with a thickness of 800 nm was spin-coated and patterned by UV lithography. This coating ensured that the sensors could be operated at voltages up to 10 V without failure or bubble formation when the sensor was exposed to ionic solutions.

During measurements, the chip was mounted in a click-on fluidic system[14] providing electrical contacts to the chip and defining a fluidic channel of dimensions length-× width × height = 5 mm × 1 mm × 1 mm (Fig. 2(a)). To align the chip with the channel and electrical contact, the chip was placed in an aluminum well (Fig. 2(b)). The temperature of the aluminum well was kept constant at (25.00 ± 0.01) °C during all measurements using a Peltier element. The set-up was neither magnetically nor electrically shielded.

Electrical measurements on the sensor were carried out using an HF2LI lock-in amplifier (Zurich Instruments, Switzerland) operating at a fixed voltage amplitude of 3.2 V corresponding to a current amplitude of $I_{AC} = 21$ mA. The 1st harmonic sensor response was measured vs. applied field resulting in a low-field sensor sensitivity of $S_0 = -531$ V/(T A).

Measurements were performed on nominally 40 nm magnetic beads with a COOH functional surface group (Ocean Nanotech, AR, USA). In this study, the bead concentration was varied from $c = 16$ μg/ml to $c = 4$ mg/ml in a 2-fold logarithmic dilution series. In the experiments, the bead concentration was varied in the following order: c [mg/ml] = 1, 0.25, 0.063, 0.5, 0.125, 0.031, 0.016, 4, 2.

Measurements on bead suspensions were carried out in ambient magnetic field where the 2nd harmonic sensor response was measured as a function of the frequency of the applied bias voltage. Each frequency sweep consisted of 20 points equally distributed on a log scale between $f = 986.9$ kHz and 37.7 Hz. After each measurement at f, a reference measurement was carried out at $f_{ref} = 4667$ Hz, which is near the expected Brownian relaxation frequency for the beads used in the experiments. Each of the above sweeps took a total time of 7 min and 20 s to complete. For each bead concentration, a cycle of 9 frequency sweeps, numbered 1–9, was performed. First, two sweeps (1 and 2) were performed without beads and were used as reference. At the start of sweep 3, beads were injected into the fluidic channel for 1 min at a flow rate of 30 μl/min. Then, the flow was stopped for the remaining part of sweep 3 and left stagnant in the following four sweeps (sweeps 4–7). At the start of sweep 8, the beads were washed out at a flow rate of 800 μl/min and sweep 9 was performed to confirm that the signal returned to its initial level from sweeps 1 and 2.

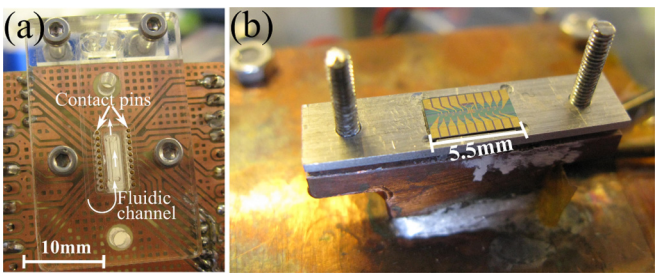

FIG. 2. (a) Fluidic system with 20 spring-loaded electrical contact pins. (b) Picture of chip in set-up prior to mounting of the fluidic system.

IV. RESULTS

A. Frequency sweeps

Figure 3 shows the in-phase (top) and out-of-phase (bottom) second harmonic sensor signals as a function of the bias current frequency for sweep 7, which is started 29 min after injection of the beads. Only measurements for the seven highest bead concentrations (63 μg/ml-4 mg/ml) are shown, as the lower concentrations are indistinguishable from $c = 63$ μg/ml on this scale. The solid lines in the figures are curve fits of the Cole-Cole model to the measured data. From Fig. 3, it is seen that the curve shape is independent of the concentration and that it scales with the bead concentration.

Figure 4 shows the Brownian relaxation frequencies f_B extracted from curve fits of the Cole-Cole model vs. bead concentration. The fits of the in-phase and out-of-phase data were carried out simultaneously with a single set of parameters. For each concentration, the values of f_B were found separately for sweeps 5–7. The error bars on each of the f_B-values in Fig. 4 correspond to the standard deviation reported by the least-squares fitting routine. It is also seen

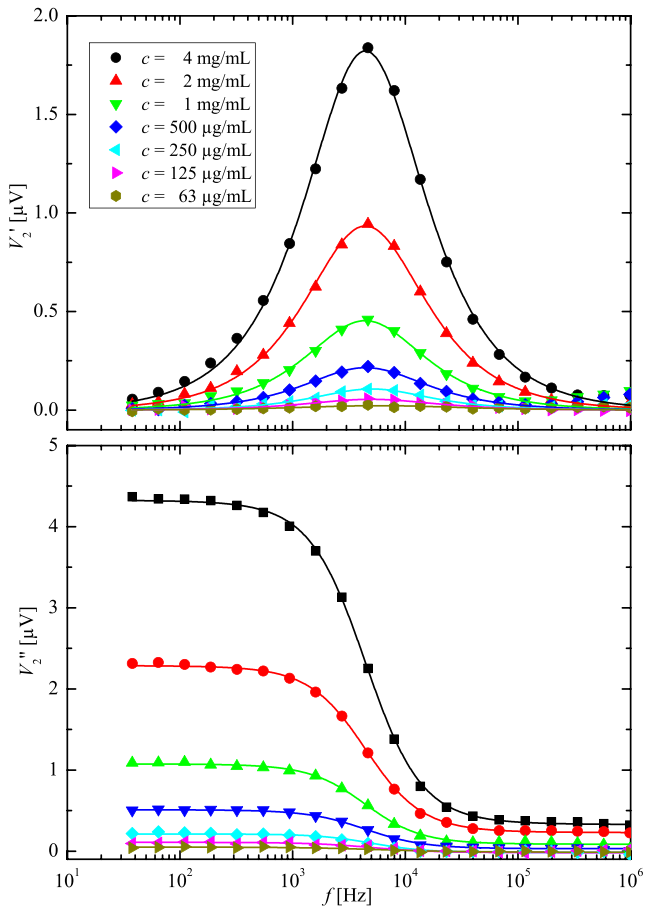

FIG. 3. In-phase (top) and out-of-phase (bottom) signals vs. bias frequency for the indicated bead suspension concentrations. The solid lines are fits of the Cole-Cole model to the measurements.

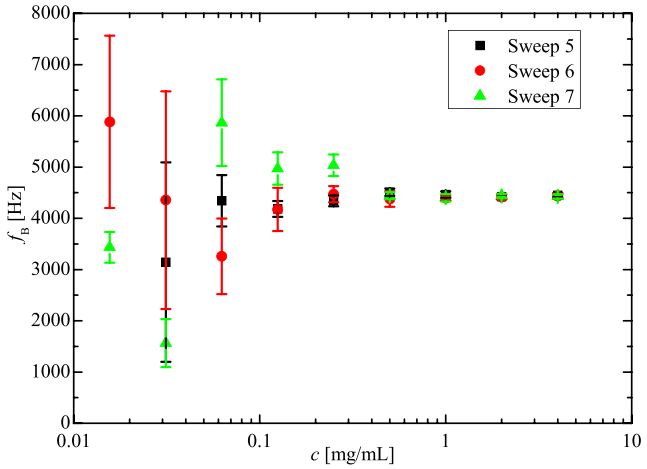

FIG. 4. Brownian relaxation frequencies extracted from sweeps 5–7 plotted against bead concentration. The length of the error bars corresponds to the standard deviations obtained from the fitting.

that for the four highest concentrations, the extracted frequencies coincide with a mean Brownian relaxation frequency of 4.4(0.1) kHz corresponding to a hydrodynamic diameter of 47(1) nm. Down to $c = 63\,\mu$g/ml the mean Brownian relaxation frequency is still 4.4 kHz, but the standard deviation increases to 0.8 kHz. The average value of the Cole-Cole parameter α was found to 0.05(0.01) for the fits shown in Fig. 4. This supports the conclusion that the curve shape is independent of the bead concentration for the investigated samples.

B. Signal at $f \simeq f_B$ vs. bead concentration

Figure 5 shows the in-phase second harmonic sensor signal of the reference points measured at $f_{ref} = 4667$ Hz normalized with c plotted vs. time t after injection of the bead suspension. The figure also shows the sweep numbers for each of the bead concentrations. Sweeps 1 and 2 are carried out without beads; the bead suspension is injected at the start of sweep 3 resulting in a signal increase and during sweeps 4–7, the signal is almost constant. During sweep 8

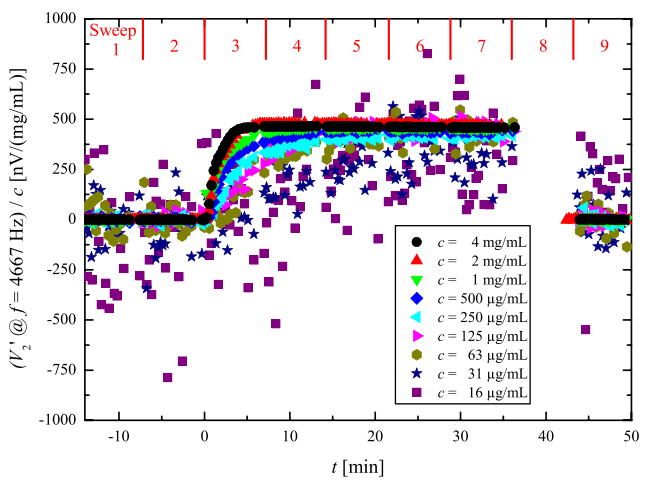

FIG. 5. In-phase 2nd harmonic sensor signal of reference points measured at $f_{ref} = 4667$ Hz normalized with bead concentration plotted as a function of the time t after injection of the bead suspension.

(not shown), the beads are washed away and the data obtained during sweep 9 shows that the signal returns to its baseline level from sweeps 1 and 2. From Fig. 5 it is observed that the signal-to-noise ratio increases with increasing bead concentration. It is also seen that a level near 460 nV/(mg/ml) is reached for all bead concentrations, except for the two lowest concentrations that are clearly at a lower level. From Fig. 5, it is also noticed that the signal rise after injection depends on the bead concentration. When the bead concentration is high, the signal reaches its steady-state value faster.

Figure 6 shows the mean values of the twenty reference points obtained during sweep 7 (last sweep before washing) as a function of the bead concentration. The error bars indicate three times the standard deviation of the mean (σ_{mean}). The line is a linear fit to the data with the intercept fixed to zero and a slope of 460(2) nV/(mg/ml). Analysis of the reference measurements obtained during sweeps 2, where the mean value defined the zero signal level in the subsequent measurements, resulted in a noise level (taken as 3 σ_{mean}) of 3.1 nV, which is shown as the horizontal dashed line in Fig. 6. It is seen that the signals from all the measured bead concentrations are significantly above the sensor noise level.

V. DISCUSSION

A. Frequency sweeps

From the frequency sweeps plotted in Fig. 3, it is seen that the shape is independent of the bead concentration, and hence that the signal scales with the concentration. This was also confirmed by the similar values of f_B and α obtained from the Cole-Cole fits for $c \geq 63\,\mu$g/ml. For the two lowest concentrations, the signal-to-noise ratio was too low to extract reliable values of f_B and α. The obtained α-value of 0.05 indicates that the bead suspension is nearly monodisperse. It is important for volume-based biodetection that the bead suspension is close to monodisperse as this results in a well defined peak in the in-phase sensor signal, which

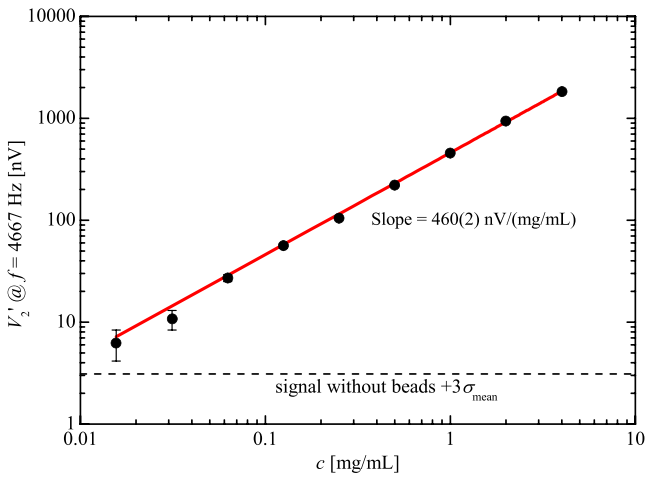

FIG. 6. Mean value of the 20 reference points measured during sweep 7 vs. bead concentration. The error bars are given as 3 σ_{mean}. The solid line is a linear fit to the data points with the intercept fixed at 0. The horizontal dashed line indicates the noise level plus 3 σ_{mean} for a measurement without any beads.

potentially allows for distinguishing the peak from isolated beads from a peak at lower frequencies due to beads bound to the target analyte.

The extracted Brownian frequencies are found to 4.4(0.8) kHz for $c \geq 63\,\mu$g/ml and 4.4(0.1) kHz for $c \geq 500\,\mu$g/ml. The mean values are identical within the uncertainties, but the standard deviation increases as the bead concentration decreases due to the lower signal-to-noise ratio. This means that if the hydrodynamic diameter needs to be extracted accurately for the present beads, a bead concentration of at least 500 μg/ml should be used.

B. Signal at $f \simeq f_B$ vs. bead concentration

Figure 5 shows the reference points measured at $f \simeq f_B$ vs. time for several bead concentrations. The values are normalized with the bead concentration and adjusted such that the injection of beads is initiated at $t = 0$ min. From this plot it is observed that the signals stabilize near 460 nV/(mg/ml) for all concentrations except for the two lowest, which do not reach this level. Figure 5 also shows that the signal returns to its baseline level after the beads are washed away, which allows for reusing the sensor.

From Fig. 5 it is seen that the rate by which the signal changes after the beads have been injected depends on the bead concentration such that a faster equilibration is found for higher bead concentrations. The equilibration arises from the fact that the bead suspension is injected into the channel containing water and that the liquid exchange near the channel wall is slower due to the parabolic velocity profile. The detailed origin of the faster equilibration for higher bead concentrations is still unknown, but we hypothesize that it could be due to cooperative phenomena, e.g., hydrodynamic interactions between the beads[20] or electrostatic repulsion between the beads due to their surface charges, which accelerate the equilibration when the bead density is high.

Figure 6 shows the average of the in-phase signal for the 20 reference points measured during sweep seven plotted vs. bead concentration. From the plot it is seen that the signal is proportional to the bead concentration with a slope of 460(2) nV/(mg/ml). It is also seen that all the measured concentrations are significantly different from reference measurement without beads on a 3 σ_{mean} level. The lowest bead mass concentration measured was 16 μg/ml, which corresponds to a particle concentration of 0.2 nM. When used in a volume-based bioassay, a lower bead concentration will increase the sensitivity and lower the dynamic range. Hence, one approach to increase the sensitivity could be to use larger magnetic beads such that the same magnetic signal can be obtained from fewer beads. However, in our system, beads that are larger than about 100 nm tend to sediment to the bottom of the fluidic channel and as the sensors are more sensitive to beads near the sensor surface, such sedimented beads will contribute significantly to the signal. The investigation of the choice of beads and optimization of the bioassay sensitivity is one focus of our future research.

VI. CONCLUSION

Based on the presented data, it is concluded that Brownian relaxation frequencies can be extracted using planar Hall effect bridge sensors for bead concentration as low as 64 μg/ml. However, a higher bead concentration results in more reliable determination of the Brownian relaxation frequency. The mean Brownian relaxation frequency for $c \geq 500\,\mu$g/ml was 4.4(0.1) kHz, which corresponds to a hydrodynamic diameter of 47(1) nm, which agrees well with the nominal size of 40 nm. The study also demonstrated that the shape of the dynamic signal is independent of the bead concentration and the amplitudes of the signals are proportional to the bead concentration once steady-state is reached. Monitoring the time dependence of the signal during bead injection showed that the signal reaches a steady state faster for higher bead concentrations. Finally, it can be concluded that the presence of beads can be detected for bead concentrations as low as 16 μg/ml.

ACKNOWLEDGMENTS

This work was supported by the Copenhagen Graduate School for Nanoscience and Nanotechnology (C:O:N:T) and the Knut and Alice Wallenberg (KAW) Foundation.

[1]A. P. Astalan, F. Ahrentorp, C. Johansson, K. Larsson, and A. Krozer, "Biomolecular reactions studied using changes in Brownian rotation dynamics of magnetic particles," Biosens. Bioelectron. **19**, 945 (2004).
[2]F. Ludwig, S. Mäuselein, E. Heim, and M. Schilling, "Magneto-relaxometry of magnetic nanoparticles in magnetically unshielded environment utilizing a differential fluxgate arrangement," Rev. Sci. Instrum. **76**, 106102 (2005).
[3]K. Enpuku, T. Minotani, T. Gima, Y. Kuroki, Y. Itoh, M. Yamashita, Y. Katakura, and S. Kuhara, "Detection of magnetic nanoparticles with superconducting quantum interference device (SQUID) magnetometer and application to immunoassays," Jpn. J. Appl. Phys., Part 2 **38**, L1102 (1999).
[4]H. Grossman, W. Myers, V. Vreeland, R. Bruehl, M. Alper, C. Bertozzi, and J. Clarke, "Detection of bacteria in suspension by using a superconducting quantum interference device," Proc. Natl. Acad. Sci. USA **101**, 129 (2004).
[5]D. R. Baselt, G. U. Lee, M. Natesan, S. W. Metzger, P. E. Sheehan, and R. J. Colton, "A biosensor based on magnetoresistance technology," Biosens. Bioelectron. **13**, 731 (1998).
[6]L. Ejsing, M. F. Hansen, A. K. Menon, H. A. Ferreira, D. L. Graham, and P. P. Freitas, "Planar Hall effect sensor for magnetic micro- and nanobead detection," Appl. Phys. Lett. **84**, 4729 (2004).
[7]S. X. Wang and G. Li, "Advances in giant magnetoresistance biosensors with magnetic nanoparticle tags: Review and outlook," IEEE T. Magn. **44**, 1687 (2008).
[8]R. S. Gaster, D. A. Hall, C. H. Nielsen, S. J. Osterfeld, H. Yu, K. E. Mach, R. J. Wilson, B. Murmann, J. C. Liao, S. S. Gambhir, and S. X. Wang, "Matrix-insensitive protein assays push the limits of biosensors in medicine," Nat. Med. **15**, 1327 (2009).
[9]A. Prieto Astalan, C. Jonasson, K. Petersson, J. Blomgren, D. Ilver, A. Krozer, and C. Johansson, "Magnetic response of thermally blocked magnetic nanoparticles in a pulsed magnetic field," J. Magn. Magn. Mater. **311**, 166 (2007).
[10]F. W. Østerberg, G. Rizzi, T. Zardán Gómez de la Torre, M. Strömberg, M. Strømme, P. Svedlindh, and M. F. Hansen, "Measurements of Brownian relaxation of magnetic nanobeads using planar Hall effect bridge sensors," Biosens. Bioelectron. **40**, 147 (2013).
[11]M. Strömberg, J. Göransson, K. Gunnarsson, M. Nilsson, P. Svedlindh, and M. Strømme, "Sensitive molecular diagnostics using volume-amplified magnetic nanobeads," Nano Lett. **8**, 816 (2008).
[12]J. Connolly and T. G. St Pierre, "Proposed biosensors based on time-dependent properties of magnetic fluids," J. Magn. Magn. Mater. **225**, 156 (2001).
[13]A. D. Henriksen, B. T. Dalslet, D. H. Skieller, K. H. Lee, F. Okkels, and M. F. Hansen, "Planar Hall effect bridge magnetic field sensors," Appl. Phys. Lett. **97**, 013507 (2010).

[14]F. W. Østerberg, B. T. Dalslet, D. Snakenborg, C. Johansson, and M. F. Hansen, "Chip-based measurements of Brownian relaxation of magnetic beads using a planar Hall effect magnetic field sensor," AIP Conf. Proc. **1311**, 176–183 (2010).
[15]B. T. Dalslet, C. D. Damsgaard, M. Donolato, M. Strømme, M. Strömberg, P. Svedlindh, and M. F. Hansen, "Bead magnetorelaxometry with an on-chip magnetoresistive sensor," Lab Chip **11**, 296 (2011).
[16]L. Neél, "Théorie du traînage magnétique des ferromagnétiques en grains fins avec applications aux terres cuites," Ann. Géophys. **5**, 99 (1949).
[17]W. Brown, "Thermal fluctuations of a single-domain particle," Phys. Rev. **130**, 1677 (1963).
[18]P. Debye, *Polar Molecules* (Chemical Catalogue Co. 1929).
[19]K. S. Cole and R. H. Cole, "Dispersion and absorption in dielectrics I. Alternating current characteristics," J. Chem. Phys. **9**, 341 (1941).
[20]C. Mikkelsen, M. F. Hansen, and H. Bruus, "Theoretical comparison of magnetic and hydrodynamic interactions between magnetically tagged particles in microfluidic systems," J. Magn. Magn. Mater. **293**, 578 (2005).